J Math Chem (2009) 45:238–256
DOI 10.1007/s10910-008-9378-3

ORIGINAL PAPER

# Higher order Morita approximations for random copolymer localization

**J. Alvarez · C. E. Soteros**

Received: 20 August 2007 / Accepted: 1 December 2007 / Published online: 26 June 2008


**Abstract** The Morita approximation is a constrained annealing procedure which yields upper bounds on the quenched average free energy for models of quenched randomness. In this article we consider a bilateral Dyck path model, first introduced by S.G. Whittington and collaborators, of the localization of a random copolymer at the interface between two immiscible solvents. The distribution of comonomers along the polymer chain is initially determined by a random process and once chosen it remains fixed. Morita approximations in which we control correlations to various orders between neighbouring monomers along the polymer chain are applied to this model. Although at low orders the Morita approximation does not yield the correct path properties in the localized region of the phase diagram, we show that this problem can be overcome by including sufficiently high-order correlations in the Morita approximation. In addition, by comparison with an appropriate lower bound, we show that well-within the localized phase the Morita approximation provides a relatively tight upper bound on the limiting quenched average free energy for bilateral Dyck path localization.

**Keywords** Random copolymer · Localization phase transition · Morita approximation · Bilateral Dyck paths · Directed walks

J. Alvarez · C. E. Soteros (✉)
Department of Mathematics and Statistics, University of Saskatchewan, 106 Wiggins Road, Saskatoon, SK, Canada S7N 5E6
e-mail: soteros@math.usask.ca

*Present Address:*
J. Alvarez
Department of Chemistry, University of Toronto, 80 St George Street, Toronto, ON, Canada M5S 3H6
e-mail: jalvarez@chem.utoronto.ca

## 1 Introduction

In this article, we consider a random copolymer as a linear polymer composed of two types of comonomers, $A$, $B$, with the sequence of $A$s and $B$s making up the polymer being determined by a random process. Once the comonomer sequence is determined it remains fixed, and hence the randomness is quenched. We consider the case that the polymer is in dilute solution with two immiscible solvents (oil and water, say) where comonomer $A$ prefers one solvent (oil, say) while comonomer $B$ prefers the other (water). There is experimental evidence that in such situations the polymer can be localized near the interface between the two solvents so that each comonomer is in its preferred solvent [1, 2]. On the other hand, at high enough temperatures, it is expected that entropic considerations will dominate and the polymer will be primarily away from and on one side of the interface, i.e. delocalized. The transition from a delocalized to a localized state is referred to as the localization phase transition for copolymers (see [3], Sect. 2.2 and references therein).

For random copolymers, the appropriate free energy is the expectation (over the monomer distribution) of the logarithm of the partition function; this is referred to as the *quenched average free energy*. In order to investigate the localization phase transition we are thus interested in the limiting (as the polymer length goes to infinity) quenched average free energy per monomer and its points of non-analyticity.

For this purpose, we investigate a directed walk model of random copolymer localization. The model is based on the self-avoiding walk model first introduced by Martin et al. [4] and Madras and Whittington [5]. However, a simpler bilateral Dyck path model is used for the configuration of the polymer. For a discussion of other models of random copolymer localization see ([3], Sect. 2.2). A closed form expression for the limiting quenched average free energy of localization is not available even for this simpler bilateral Dyck path model. Instead we investigate a sequence of upper bounds on the limiting quenched average free energy obtained using Morita approximations.

Recently, Alvarez et al. [6] developed a sequence of Morita upper bounds on the limiting quenched average free energy for Dyck and Motzkin path models of random copolymer adsorption. Well-within the adsorbed region of the phase diagram, they showed that by including higher and higher orders of correlations the Morita approximation upper bounds on the limiting quenched average free energy become increasingly better and even at small orders are already tight bounds. In this article, we adapt the direct renewal arguments introduced in [6] to obtain a sequence of Morita upper bounds on the limiting quenched average free energy for the localization of bilateral Dyck paths.

The annealed and first-order Morita approximations for bilateral Dyck path localization are well-understood [7, 8]. At these low orders the Morita approximation does not yield the correct path properties in the localized region of the phase diagram. In particular, for the first-order Morita a phase consisting of a mixture of the two delocalized phases can exist [7]. We show that this problem can be overcome by including sufficiently high-order correlations in the Morita approximation. In addition, by comparison with an appropriate lower bound, we show that well-within the localized phase the Morita approximation provides a relatively tight upper bound on the limiting quenched average free energy for bilateral Dyck path localization.

The article is organized as follows. The model is introduced in Sect. 2. A review of the annealed and first-order Morita results of [7, 8] is given in Sect. 3. Precise definitions of the terms "mixture phase" and "truly localized phase" are also given in Sect. 3. The background and notation needed to explain higher order Morita approximations is presented in Sect. 4. The application of the direct renewal Morita approach to bilateral Dyck path localization is discussed in Sect. 5. In Sect. 6, expressions for the mixture phase free energy are presented, and then results and conclusions are given, respectively, in Sects. 7 and 8.

## 2 The localization model and bilateral Dyck paths

A *bilateral Dyck path* [7, Fig. 1] is a walk in two dimensions which

1. starts at the origin and ends on the line $y = 0$ and
2. has steps (of length $\sqrt{2}$) only in the directions $(1, 1)$ and $(1, -1)$.

In bilateral Dyck path models for localization, any path $\omega$ of length $n$ can be represented by the sequence $\omega = (\omega_0, \omega_1, \ldots, \omega_n)$, where $\omega_i$ represents the $i$th vertex of the path having $x$-coordinate $i$ and $y$-coordinate $\omega_i$. A vertex with $y = 0$ is called a *visit*. Consider a sequence of i.i.d. Bernoulli random variables $\chi = (\chi_1, \chi_2, \ldots, \chi_n)$ and associate it with the path $\omega$ by assigning the *colour* $\chi_i \in \{0, 1\}$ to vertex $i$. ($\chi_i = 1$ corresponds to comonomer $A$ at vertex $i$.) Let $p$ be the probability that $\chi_i = 1$. For $j \in \{-1, 0, 1\}$, let $\Delta_i^j(\omega)$ be a function that indicates the location of the $i$th vertex of $\omega$ relative to the interface, i.e. $\Delta_i^j(\omega) = 1$ if the sign of $\omega_i$ = sign of $j$ (the case $j = 0$ indicates a visit at vertex $i$) and $\Delta_i^j(\omega) = 0$ otherwise; let $\Delta^j(\omega) = (\Delta_i^j(\omega), i = 1, \ldots, n)$. Using the model from [5] (see also [7, 8]), the appropriate partition function for the set, $\Omega_n$, of $n$-step bilateral Dyck paths and fixed $\chi$, is then

$$Z_n(\alpha, \beta, \gamma|\chi) = \sum_{\omega \in \Omega_n} \exp\left(H(\alpha, \beta, \gamma, \omega|\chi)\right) \tag{1}$$

with the Hamiltonian

$$H(\alpha, \beta, \gamma, \omega|\chi) = \alpha \sum_{i=1}^{n} \chi_i \Delta_i^{+1}(\omega) + \beta \sum_{i=1}^{n} (1 - \chi_i)\Delta_i^{-1}(\omega) + \gamma \sum_{i=1}^{n} \Delta_i^0(\omega). \tag{2}$$

The corresponding free energy per monomer is $\kappa_n(\alpha, \beta, \gamma|\chi) = n^{-1} \log Z_n(\alpha, \beta, \gamma|\chi)$ and it is known that the *limiting quenched average free energy*,

$$\bar{\kappa}(\alpha, \beta, \gamma) = \lim_{n\to\infty} \langle \kappa_n(\alpha, \beta, \gamma|\chi)\rangle \equiv \lim_{n\to\infty} \bar{\kappa}_n(\alpha, \beta, \gamma) \tag{3}$$

exists where the average is taken over the distribution of $\chi$ [5]. (The argument given in [5] (see also [9], Lemma 1) is for self-avoiding walks but applies *mutatis mutandis* for bilateral Dyck paths.)

If the only contribution to the partition function was from paths having all but the first and last of their vertices above (below) the interface, then the corresponding limiting quenched average free energy would be given by $d_A(\alpha) = \alpha p + \log 2$ ($d_B(\beta) = \beta(1-p) + \log 2$). Given a point $(\alpha, \beta, \gamma)$, if $\bar{\kappa}_n(\alpha, \beta, \gamma) = d_A(\alpha)$ ($d_B(\beta)$), then we say the system is *delocalized-above* (*-below*) at $(\alpha, \beta, \gamma)$. Also, as in [5], we say the system is *delocalized* at $(\alpha, \beta, \gamma)$ if $\bar{\kappa}_n(\alpha, \beta, \gamma) = \max\{d_A(\alpha), d_B(\beta)\}$ and otherwise the system is considered *localized*. Given fixed $\gamma$, one can then define

$$\beta_c(\alpha, \gamma) = \sup\{\beta | \bar{\kappa}_n(\alpha, \beta, \gamma) = \alpha p + \log 2\}, \tag{4}$$

with $\beta_c(\alpha, \gamma) \equiv -\infty$ if the set on the right-hand-side is empty. Applying the self-avoiding walk arguments from [5] along with bounds obtained from the first-order Morita approximation [8], it is then possible to prove the following for the localization phase diagram of random copolymer bilateral Dyck paths.

(i) There exists $\gamma_L$, bounded by $\max\{\log[2/p], \log[2/(1-p)]\} \leq \gamma_L \leq (\log 2)(\max\{2/p, 2/(1-p)\})$, such that for any $\gamma > \gamma_L$ and for any $\alpha, \beta$ the system is localized, while for $\gamma < \gamma_L$ the delocalized phase exists.

(ii) For any fixed value of $\gamma$, at every point on the line $\beta = \alpha p/(1-p)$, except $\alpha = \beta = 0$ for $\gamma \leq 0$, the system is localized and the limiting quenched average density of visits, $\lim_{n\to\infty} \left\langle \sum_{i=1}^{n/2} \Delta_{2i}^0(\omega) \right\rangle / n$, is non-zero.

(iii) For any fixed value of $\gamma < \gamma_L$, the phase boundary $\beta = \beta_c(\alpha, \gamma) \leq \alpha p/(1-p)$ in the $(\alpha, \beta)$-plane between the localized and delocalized-above phases exists (i.e. there exists $\alpha$ such that $\beta_c(\alpha, \gamma) > -\infty$). Also, $\beta_c(\alpha, \gamma)$ is a non-decreasing, concave function of $\alpha$ and is therefore continuous in $\alpha$. There is a symmetry related phase boundary between the localized and delocalized-below phases that lies above the line $\beta = p\alpha/(1-p)$.

(iv) For any fixed $\gamma \leq 0$, $\beta_c(0, \gamma) = 0$ and the transition between the two delocalized phases is first order at $(0, 0, \gamma)$.

In (ii), we have also used the fact that, for any $\gamma > 0$ the point $(0, 0, \gamma)$ is in the interior of the localized phase for bilateral Dyck paths. This comes from the fact that $\bar{\kappa}(0, 0, \gamma)$ equals the limiting free energy for adsorbing homopolymer bilateral Dyck paths at a penetrable surface, and hence $\bar{\kappa}(0, 0, \gamma) = d_A(0) = d_B(0) = \log 2$ for $\gamma \leq 0$ and $\bar{\kappa}(0, 0, \gamma) > \log 2$ for $\gamma > 0$ [10, Sect. 2.3].

These properties, together with a lower bound (such as that presented here in Eq. 35) establish that the phase boundary has a horizontal asymptote. See [5] for schematic figures of the phase boundary when $\gamma \leq 0$ [5, Fig. 1] and when $\gamma > 0$ [5, Fig. 2].

## 3 Annealed and first-order Morita approximations for bilateral Dyck paths

The localization problem for randomly coloured bilateral Dyck paths has been investigated in the annealed approximation and also in a Morita approximation in which the first moment of the colour distribution is fixed [7, 8]. For the annealed approximation the limiting annealed free energy, $\lim_{n\to\infty} n^{-1} \log\langle Z_n(\alpha, \beta, \gamma | \chi)\rangle$, is a simple linear transform of the homopolymer limiting free energy and, although it provides an upper

bound on the limiting quenched average free energy, it does not display all the known properties of the quenched phase diagram. For example, for $\gamma = 0$ and $\alpha > 0$ property (ii) above does not hold for the annealed model, but rather the line $\beta = \alpha p/(1-p)$ forms a phase boundary between the two delocalized phases [7]. Furthermore, the delocalized limiting annealed average free energy is $\max\{\log(p\exp(\alpha)+1-p), \log(p+(1-p)\exp(\beta))\} + \log 2$, which is different from the delocalized limiting quenched average free energy, $\max\{d_A(\alpha), d_B(\beta)\}$. However, for example for $p = 1/2$, fixed $\gamma$ and $\beta \le \alpha \le \log(2\exp(\gamma) - 1)$, there exists a delocalized-localized phase boundary given by

$$\beta = \beta_a(\alpha, \gamma) = \log\left(\frac{1 - 4\,e^{\gamma} + 2e^{\alpha} + 2e^{2\,\gamma+\alpha} - 6e^{\gamma+\alpha} + 4e^{2\,\gamma} + e^{2\alpha} - 2\,e^{\gamma+2\,\alpha}}{2\,e^{\gamma} - 2\,e^{2\,\gamma} + 2\,e^{\gamma+\alpha} - 2\,e^{\alpha} - e^{2\,\alpha} - 1}\right) \tag{5}$$

which is consistent with property (iii). For $p = 1/2$ and any fixed $\gamma$, the two delocalized phases coincide along the line $\alpha = \beta$ for all $\beta \ge \log(2\exp(\gamma) - 1)$. (See [7, Fig. 4] for these delocalized phase boundaries at $\gamma = 0$). Corresponding expressions are known for general $p$.

The situation with respect to property (ii) improves by introducing a constraint on the first moment of the colour distribution, namely $\left\langle \sum_i \chi_i \right\rangle = np$; this gives a first-order Morita approximation. With this constraint, every point on the line $\beta = \alpha p/(1-p)$, except $\alpha = \beta = 0$ for $\gamma \le 0$, is now localized, consistent with property (ii). However, the limiting average density of visits can be zero along this line, and hence property (ii) only partially holds true. More specifically, the limiting first-order Morita free energy is given by

$$\kappa_1(\alpha, \beta, \gamma) = \lim_{n\to\infty} n^{-1} \log\left\langle Z_n(\alpha, \beta, \gamma|\chi) \exp\left(\lambda^* \sum_i (\chi_i - p)\right)\right\rangle, \tag{6}$$

where $\lambda^*$ is chosen to ensure that the first moment of the colour distribution is constrained correctly. In this case, the delocalized phase free energy has the correct value $\max\{d_A(\alpha), d_B(\beta)\}$ and, for $\gamma < \log[2/(1-p)]$, there exists a finite localized-delocalized-above phase boundary $\beta = \beta_1(\alpha, \gamma) = \sup\{\beta|\kappa_1(\alpha, \beta, \gamma) = d_A(\alpha)\}$ in the $(\alpha, \beta)$-plane. For $p = 1/2$,

$$\beta_1(\alpha, \gamma) = \begin{cases} \log\left(\frac{c^2+8\,a^2+2\,c^2a^3-8\,a^3c-12\,a^2c+5\,a^2c^2-4\,ca+4\,c^2a}{a(-8\,a^2+4\,a^2c-a^2c^2-2\,c^2a+4\,ca-c^2)}\right) & a < c/(2-c) \\ \log(2 - 1/a) & a \ge c/(2-c) \end{cases} \tag{7}$$

where $a = e^{\alpha}$ and $c = e^{\gamma}$. This differs from the annealed phase boundary, $\beta = \beta_a(\alpha, \gamma)$, as in Eq. 5. Corresponding expressions are known for general $p$. For any $\alpha \ne 0$, $\beta_1(\alpha, \gamma) < \alpha p/(1-p)$, which is consistent with property (ii). Consistent with property (iii), there is also a symmetry related localized-delocalized-below phase boundary. (See [7, Fig. 5] for these delocalized phase boundaries at $\gamma = 0$.) Furthermore, consistent with property (i), there exists $\gamma_L^{(1)} = \max\{\log[2/(1-p)], \log[2/p]\}$

such that the whole $(\alpha, \beta)$-plane is localized for all $\gamma > \gamma_L^{(1)}$ while for $\gamma < \gamma_L^{(1)}$ the delocalized phase exists.

However, in contrast to the expected quenched phase behaviour, now there exist two types of localized phases which are separated from each other by a third phase boundary. For example for $\gamma = 0$ and $\alpha > 0$, the line $\beta = \alpha p/(1-p)$ lies within a region where the system is localized, since $\kappa_1(\alpha, \beta, \gamma) > \max\{d_A(\alpha), d_B(\beta)\}$, but the limiting density of visits, $\lim_{n\to\infty}\langle\sum_i \Delta_{2i}^0(\omega)\rangle/n$, is zero. This is a region in which the two delocalized phases coexist and we refer to this phase as the *mixture* phase. This coexistence region is defined by $a > p/(1-b(1-p))$ and $b > (1-p/a)/(1-p)$, where $a = e^{\alpha}$ and $b = e^{\beta}$ [7]. Again for $\gamma = 0$ but now with $\alpha < 0$, the line $\beta = \alpha p/(1-p)$ lies within a region where the system is localized and in which the limiting density of visits is strictly positive. As this is the expected path behaviour for the quenched system (see property (ii)), we refer to this phase as the *truly localized* phase. Furthermore, for any fixed $\gamma > -\log 2$, along the line $\beta = \alpha p/(1-p)$ there exists a critical value $\alpha^*$ such that for all $0 \le \alpha < \alpha^*$ the system is truly localized while for $\alpha > \alpha^*$ the system is in the mixture phase. In fact, $(\alpha^*, \alpha^* p/(1-p), \gamma)$ is one point on a phase boundary, $\beta = \beta_m^{(1)}(\alpha, \gamma)$, between a truly localized region and the mixture phase [8]. For $(\alpha, \beta, \gamma)$ in the localized region,

$$\beta_m^{(1)}(\alpha, \gamma) = \log\left(\frac{-e^{\gamma+\alpha} - 1 + 2\,e^{\gamma}}{-e^{\alpha} + e^{\gamma}}\right). \tag{8}$$

In Fig. 1, the first-order Morita approximation phase boundaries are plotted in the $(\alpha, \beta)$-plane for $p = 1/2$ and various values of $\gamma$. In Fig. 1a, $\gamma = 1.5 > \gamma_L^{(1)}$ and hence the whole plane is localized, however, both the truly localized (including the origin) and mixture phases exist and are separated by the phase boundary $\beta = \beta_m^{(1)}(\alpha, \gamma)$ as plotted. Figure 1a represents the typical situation for any $\gamma \ge \gamma_L^{(1)} = 2\log 2$. In Fig. 1b–e, all three phase boundaries exist. Figure 1b is for $\gamma = 0.85$ and this represents the typical situation for any $\log 2 \le \gamma < \gamma_L^{(1)}$. Figure 1c is for $\gamma = 0.63$ and this represents the typical situation for any $0 < \gamma < \log 2$. Figure 1d is for $\gamma = -0.3$ and this represents the typical situation for any $\log(2/3) < \gamma < 0$. Figure 1e is for $\gamma = -0.5$ and this represents the typical situation for any $-\log 2 < \gamma \le \log(2/3)$. In Fig. 1f, $\gamma = -0.75$ and the phase boundary $\beta = \beta_m^{(1)}$ no longer exists. Instead, the whole localized region consists of the mixture phase. This represents the typical situation for $\gamma \le -\log 2$. Note that at $\gamma = 0$, the phase boundaries are as depicted in Fig. 1f, however, the localized phase in the third quadrant is a truly localized phase. The concavity of the phase boundary $\beta = \beta_m^{(1)}(\alpha, \gamma)$ changes sign from $\gamma < 0$ to $\gamma > 0$.

The existence of the mixture phase can be attributed to the fact that the first moment constraint is satisfied by placing $pn$ of the vertices in the walk above the interface and colouring them $A$, and placing the remaining $(1-p)n$ vertices below and colouring them $B$. Thus the free energy can be optimized and the moment constraint satisfied without having to consider walks which cross the interface more than once. One expects that if further constraints on the colour distribution are introduced then the mixture phase will be replaced by a truly localized phase. Since the first order Morita

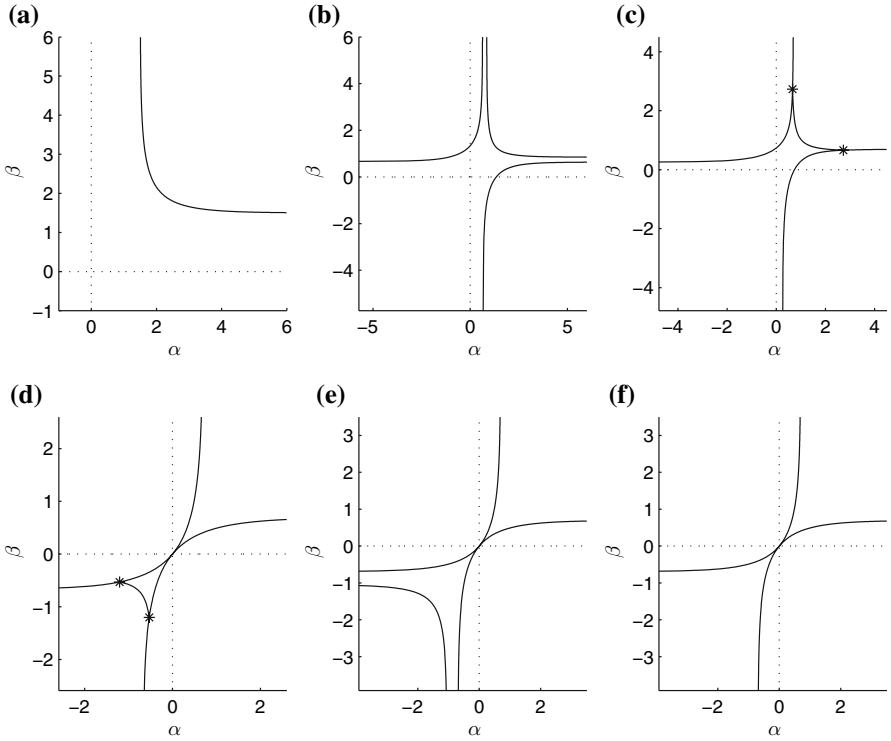


**Fig. 1** The first-order Morita phase boundaries in the $(\alpha, \beta)$-plane for: (**a**) $\gamma = 1.5$, (**b**) $\gamma = 0.85$, (**c**) $\gamma = 0.63$, (**d**) $\gamma = -0.3$, (**e**) $\gamma = -0.5$, and (**f**) $\gamma = -0.75$

does yield the correct delocalized free energy, the critical curve, $\beta_1(\alpha, \gamma)$, bounding the delocalized-above region is not expected to change by including more constraints in a Morita approximation [11]. However, the bound on the limiting quenched average free energy can be improved. Thus we investigate higher order Morita approximations to determine what constraints are needed to yield a truly localized phase instead of a mixture. To do this, we first introduce some background and notation about Morita approximations.

## 4 Higher order Morita approximations for bilateral Dyck paths

The results of Morita [12] and others [13, 14] show that the quenched average free energy can be obtained by the constrained optimization of an annealed free energy. To see this, one considers a set of Lagrange multipliers $\lambda = (\lambda_C, \forall C \subseteq \{1, 2, \ldots, n\}) \in \mathbb{R}^{2^n}$ and the corresponding partition function

$$\hat{Z}_n(\alpha, \beta, \gamma, \lambda|\chi) = Z_n(\alpha, \beta, \gamma|\chi)e^{\Lambda(\lambda|\chi)}, \tag{9}$$

where for each subset $C$ of vertices, $\Lambda(\lambda|\chi)$ is used to impose the correct distribution for the probability that exactly the vertices in $C$ are coloured $A$. Specifically,

$$\Lambda(\lambda|\chi) = \sum_{C\neq\emptyset} \lambda_C \left[ \left( \prod_{i\in C} \chi_i \prod_{i\notin C} (1-\chi_i) \right) - p^{|C|}(1-p)^{n-|C|} \right] \tag{10}$$

and the sum is over all $C \subseteq \{1, 2, \ldots, n\}$. Minimizing $n^{-1}\log\langle\hat{Z}_n(\alpha, \beta, \gamma, \lambda|\chi)\rangle$ with respect to the $\lambda_C$'s yields the quenched average free energy $\bar{\kappa}_n(\alpha, \beta, \gamma)$ for the model and ensures that the colour distribution constraint is satisfied for each subset $C \neq \emptyset$ [3]. That is, the minimization ensures that $\frac{\partial}{\partial\lambda_C}\log\langle\hat{Z}_n(\alpha, \beta, \gamma, \lambda|\chi)\rangle = 0$ and hence for each choice of $C \subseteq \{1, \ldots, n\}$

$$\left\langle \prod_{i\in C} \chi_i \prod_{i\notin C} (1-\chi_i) \right\rangle = p^{|C|}(1-p)^{n-|C|}. \tag{11}$$

A *Morita approximation*, $\kappa_n^M(\alpha, \beta, \gamma)$, for $\bar{\kappa}_n(\alpha, \beta, \gamma)$ is obtained by relaxing some of these constraints (in the annealed case, all the $\lambda_C$'s are set to zero). Minimizing $n^{-1}\log\langle\hat{Z}_n(\alpha, \beta, \gamma, \lambda|\chi)\rangle$ with respect to the reduced set, $\lambda^M$, of $\lambda_C$'s yields an upper bound on $\bar{\kappa}_n(\alpha, \beta, \gamma)$ for the model, i.e. $\kappa_n^M(\alpha, \beta, \gamma) = \min_{\lambda^M} n^{-1}\log\langle\hat{Z}_n(\alpha, \beta, \gamma, \lambda^M|\chi)\rangle \geq \bar{\kappa}_n(\alpha, \beta, \gamma)$. The minimization is typically quite complicated, however, one can also obtain an upper bound $\kappa_U(\alpha, \beta, \gamma)$ on $\bar{\kappa}(\alpha, \beta, \gamma)$ via

$$\begin{aligned}\kappa_U(\alpha, \beta, \gamma) &= \min_{\lambda^M} \lim_{n\to\infty} \frac{1}{n}\log\langle\hat{Z}_n(\alpha, \beta, \gamma, \lambda^M|\chi)\rangle \\ &= \min_{\lambda^M} \left\{ -\log\left(r_G(\alpha, \beta, \gamma, \lambda^M)\right) \right\} \geq \lim_{n\to\infty} \kappa_n^M(\alpha, \beta, \gamma) \geq \bar{\kappa}(\alpha, \beta, \gamma)\end{aligned} \tag{12}$$

where $r_G(\alpha, \beta, \gamma, \lambda^M)$ is the radius of convergence of the generating function

$$G(z, \alpha, \beta, \gamma, \lambda^M) = \sum_{n=0}^{\infty} z^n \langle\hat{Z}_n(\alpha, \beta, \gamma, \lambda^M|\chi)\rangle. \tag{13}$$

We use the term "order" with respect to a Morita approximation to reflect the extent to which the colour distribution is constrained in the approximation. In particular, we say a Morita approximation has *order* $\sigma \geq 1$ when $\sigma - 1$ is the maximum distance between vertices in a colour distribution constraint of the approximation. The annealed approximation is referred to as the zeroth order Morita approximation.

For both the annealed and first-order Morita approaches discussed in the previous section, $G(z, \alpha, \beta, \gamma, \lambda^M)$ can be expressed in terms of a homopolymer generating function which keeps track of the number of visits and the number of steps above the interface in the walks. Thus (in principle) the Morita limiting free energy can

be obtained from a re-parametrization of the well-known singularity structure of the homopolymer model [7, 8].

For higher order Morita approximations, by using a direct renewal approach (as introduced in [6] for random copolymer adsorption of Dyck paths), it is still possible to relate $G(z, \alpha, \beta, \gamma, \lambda^M)$ to a homopolymer generating function that will however now be a more complicated function of the paths involved. We discuss some of the details of this next.

## 5 Direct renewal for bilateral Dyck path Morita approximations

The standard factorization (or renewal) arguments for directed paths take advantage of the fact that after the first return to the surface the remaining portion of the path is again a directed path. However, correlation constraints such as $\langle \chi_i \chi_{i+1} \rangle = p^2, i = 1, \ldots, n-1$ are complicated to factor at the location of the first return to the surface. This difficulty can be reduced by considering only colouring constraints on non-overlapping vertex sequences. In fact, given an order $\sigma \geq 1$, for each $i \geq 0$, for our approximation the full set of colouring constraints, Eq. 11, is imposed on the vertices $(i\sigma + j, j = 1, \ldots, \sigma)$. Note that these sequences of vertices do not overlap. This has the advantage that we can write the partition function almost immediately in terms of a homopolymer partition function. We explain this in more detail now but limit our discussion to the case $\sigma = 2$ and refer to a subsequent paper for the full details and the generalization to higher values of even $\sigma$.

Note that for the quenched problem the distribution of $\chi_i$ is fixed. Hence the $\chi_i$, $i = 1, \ldots, n$, are i.i.d. Bernoulli and the colour distribution constraints in Eq. 11 are automatically satisfied in the quenched average. However, for a Morita approximation, the colouring and the walk configurations are assumed to change on the same time scale and only those constraints in Eq. 11 which are imposed in the approximation are guaranteed to hold in the constrained annealed average.

For the direct renewal Morita approximation with $\sigma = 2$ and $n = 2k$, we decompose the colouring $\chi$ into $k$ subcolourings each of length $\sigma$:

$$\underbrace{\chi_1, \chi_2}_{\chi^{(1)}} \cdots \underbrace{\chi_{2i-1}, \chi_{2i}}_{\chi^{(i)}} \cdots \underbrace{\chi_{2k-1}, \chi_{2k}}_{\chi^{(k)}}.$$

Then we assume that in the constrained annealed average the $\chi^{(i)} = (\chi_1^{(i)}, \chi_2^{(i)})$, $i = 1, \ldots, k$, are independent and identically distributed such that for each $i$:

$$\langle (1 - \chi_1^{(i)})(1 - \chi_2^{(i)}) \rangle = (1-p)^2 \tag{14}$$

$$\langle (1 - \chi_1^{(i)}) \chi_2^{(i)} \rangle = p(1-p) \tag{15}$$

$$\langle \chi_1^{(i)} (1 - \chi_2^{(i)}) \rangle = p(1-p) \tag{16}$$

$$\langle \chi_1^{(i)} \chi_2^{(i)} \rangle = p^2. \tag{17}$$

But otherwise the colour distribution is unconstrained. We refer to Eqs. 14–17 as the *full set of colour distribution constraints* for the vertices $(2i + j,\ j = 1, 2)$. To impose these for a given $i$, a separate Lagrange multiplier, $\lambda_0, \ldots, \lambda_3$, is introduced for the respective constraints Eqs. 14–17. Then, due to the i.i.d. assumption on the $\chi^{(i)}$, the same set of multipliers is used for each $i = 1, \ldots, k$. (Note that any three of the constraints in Eqs. 14–17 implies the fourth, however, for simplicity we include a Lagrange multiplier for each constraint).

Let $\lambda = (\lambda_0, \ldots, \lambda_3)$, thus the Lagrangian for the second order direct renewal Morita approximation is given by

$$\begin{aligned}\Lambda^{(2)}(\lambda|\chi) &= \lambda_0 \sum_{i=1}^{k}[(1-\chi_1^{(i)})(1-\chi_2^{(i)}) - (1-p)^2] \\ &\quad +\lambda_1 \sum_{i=1}^{k}[(1-\chi_1^{(i)})\chi_2^{(i)} - p(1-p)] \\ &\quad +\lambda_2 \sum_{i=1}^{k}[\chi_1^{(i)}(1-\chi_2^{(i)}) - p(1-p)] + \lambda_3 \sum_{i=1}^{k}[\chi_1^{(i)}\chi_2^{(i)} - p^2] \qquad (18) \\ &= -k[\lambda_0(1-p)^2 + (\lambda_1+\lambda_2)p(1-p) + \lambda_3 p^2] \\ &\quad + \sum_{i=1}^{k}\Big[\lambda_0(1-\chi_1^{(i)})(1-\chi_2^{(i)}) + \lambda_1(1-\chi_1^{(i)})\chi_2^{(i)} + \lambda_2\chi_1^{(i)}(1-\chi_2^{(i)}) \\ &\quad +\lambda_3\chi_1^{(i)}\chi_2^{(i)}\Big]. \qquad (19)\end{aligned}$$

Note that for a given $\chi$ and $i$, there is only one non-zero term in the rightmost summand of Eq. 19 and that corresponds to $\lambda_j$ where $j$ is the order, $o(i)$, of the colouring $\chi^{(i)} = (\chi_{2i-1}, \chi_{2i})$ in a lexicographic ordering of the colourings in $\{0, 1\}^2$. Thus

$$\Lambda^{(2)}(\lambda|\chi) = -nq^{(2)}(\lambda) + \sum_{i=1}^{n/2}\lambda_{o(i)}, \qquad (20)$$

where

$$q^{(2)}(\lambda) = \frac{1}{2}\left(\lambda_3 p^2 + \lambda_2 p(1-p) + \lambda_1(1-p)p + \lambda_0(1-p)^2\right) \qquad (21)$$

is independent of $\chi$. Thus the second-order direct renewal Morita approximation average partition function is given by

$$\langle Z_n^{(2)}(\alpha, \beta, \gamma, \lambda|\chi)\rangle = \sum_{\chi} p^{\sum_i \chi_i}(1-p)^{n-\sum_i \chi_i} Z_n(\alpha, \beta, \gamma|\chi) e^{\Lambda^{(2)}(\lambda|\chi)} \qquad (22)$$

$$= e^{-nq^{(2)}(\lambda)} \sum_{\omega\in\Omega_n} \prod_{i=1}^{n/2} \Big[ p^2 e^{\alpha(\Delta_{2i-1}^{+1}(\omega)+\Delta_{2i}^{+1}(\omega))+\gamma\Delta_{2i}^{0}(\omega)+\lambda_3}$$
$$+p(1-p)e^{\alpha\Delta_{2i-1}^{+1}(\omega)+\beta\Delta_{2i}^{-1}(\omega)+\gamma\Delta_{2i}^{0}(\omega)+\lambda_2}$$
$$+(1-p)pe^{\alpha\Delta_{2i}^{+1}(\omega)+\beta\Delta_{2i-1}^{-1}(\omega)+\gamma\Delta_{2i}^{0}(\omega)+\lambda_1}$$
$$+(1-p)^2 e^{\beta(\Delta_{2i-1}^{-1}(\omega)+\Delta_{2i}^{-1}(\omega))+\gamma\Delta_{2i}^{0}(\omega)+\lambda_0} \Big]. \tag{23}$$

The term in the square brackets depends only on the sequence of 2-tuples $t_i(\omega) = (\Delta_{2i-1}^{+1}(\omega), \Delta_{2i}^{+1}(\omega)), (\Delta_{2i-1}^{-1}(\omega), \Delta_{2i}^{-1}(\omega)), (\Delta_{2i-1}^{0}(\omega), \Delta_{2i}^{0}(\omega))$. Note that odd vertices cannot be visits so $\Delta_{2i-1}^{0}(\omega) = 0$, and any even vertex, $\omega_{2i}$, is limited to being either a visit or on the same side of the interface as $\omega_{2i-1}$. Thus $t_i$ is determined by the choice of $j \in \{-1, 1\}$ such that $\Delta_{2i-1}^{j}(\omega) = 1$ and the choice of $\Delta_{2i}^{0}(\omega) \in \{0, 1\}$, and hence $t_i$ has only four possible states. In fact $t_i$ is completely determined by $s^{(i)}(\omega) = (\Delta_{2i-1}^{-1}(\omega), \Delta_{2i}^{0}(\omega))$. Thus the term in the square brackets in Eq. 23 has four possible values, $w_j$, $j = 0, \ldots, 3$,

$$w_j = e^{\gamma s_0} \Big[ p^2 e^{\alpha(1-s_1)(2-s_0)+\lambda_3} + p(1-p)e^{\alpha(1-s_1)+\beta s_1(1-s_0)+\lambda_2}$$
$$+(1-p)pe^{\alpha(1-s_1)(1-s_0)+\beta s_1+\lambda_1} + (1-p)^2 e^{\beta s_1(2-s_0)+\lambda_0} \Big] \tag{24}$$

with the sequence $s_1 s_0$ given by the bits in $j$ base 2. When the term in the square brackets equals $w_j$ (i.e. when $s^{(i)}(\omega) = (s_1, s_0)$), then we say that the $i$th subsequence, $\omega^{(i)} = \omega_{2i-1}\omega_{2i}$, of the walk is type $j$.

Hence, by grouping together all the walks that have the same numbers of subsequences of each of the four types one now obtains

$$G^{(2)}(z, \alpha, \beta, \gamma, \lambda) = \sum_{n\geq 0} z^n \langle Z_n^{(2)}(\alpha, \beta, \gamma, \lambda|\chi)\rangle = B^{(2)}(ze^{-q^{(2)}(\lambda)}, w_0, \ldots, w_3) \tag{25}$$

where $B^{(2)}(x_0, x_1, x_2, x_3, x_4)$ is the generating function

$$B^{(2)}(x_0, x_1, \ldots, x_4) = \sum_{n\geq 0} x_0^n \sum_{m_1,\ldots,m_4} b_n(m_1, \ldots, m_4) \prod_{j=1}^{4} x_j^{m_j} \tag{26}$$

for the number, $b_n(m_1, \ldots, m_4)$, of $n$-edge bilateral Dyck paths with $m_j$ of its subsequences being type $j$. $B^{(2)}(x_0, x_1, x_2, x_3, x_4)$ can be determined exactly using standard renewal (factorization) arguments, and we leave the details of that to a subsequent paper.

For each even $\sigma \geq 1$, the same procedure results in a homopolymer generating function, $B^{(\sigma)}$, from which it is possible to compute an upper bound $\kappa_U^{(\sigma)}(\alpha, \beta, \gamma)$ via Eq. 12. The upper bound is in terms of the singularities of $B^{(\sigma)}$. Indeed the radius of convergence of $G^{(\sigma)}(z, \alpha, \beta, \gamma, \lambda)$ will satisfy the inequality

$$r_G(\alpha, \beta, \gamma, \lambda) \geq e^{q^{(\sigma)}(\lambda)} \min\left\{|z_1|, |z_2|, \ldots, |z_{2+n_r}|\right\} \tag{27}$$

where $z_3, \ldots, z_{2+n_r}$ are the poles of $B^{(\sigma)}$ while $z_1$ and $z_2$ are square root singularities governing the two delocalized phases. The $z_i$'s are functions of $\alpha, \beta, \gamma$ and $\lambda$. Therefore from Eq. 12, the upper bound $\kappa_U^{(\sigma)}(\alpha, \beta, \gamma)$ becomes

$$\kappa_U^{(\sigma)}(\alpha, \beta, \gamma) = \max_{\lambda} \left\{q^{(\sigma)}(\lambda) + \min\{\log|z_1|, \log|z_2|, \ldots, \log|z_{2+n_r}|\}\right\}. \tag{28}$$

Closed form expressions for the $z_i$'s are available for $\sigma = 1$ and $\sigma = 2$ for bilateral Dyck paths. For these choices of $\sigma$ it is possible to determine $\kappa_U^{(\sigma)}$ either exactly or by numerical optimization, depending on the values of $\alpha, \beta, \gamma$. In particular, it is still possible to determine the delocalized phase boundaries exactly for these values of $\sigma$, and they do not change from first order to second order as expected [11]. For higher values of $\sigma$, determining $z_2, \ldots, z_{1+n_r}$ involves finding the roots of a polynomial of degree greater than five. Hence the roots can only be determined numerically for specific choices of $\lambda, \alpha, \beta, \gamma$ and thus the optimization must also be done numerically.

## 6 The mixture free energy

As mentioned above, one of the goals of considering higher order Morita approximations is to find an approximation which fully satisfies property (ii), i.e. which is truly localized along the line $\beta = \alpha p/(1-p)$ except at $\alpha = \beta = 0$ for $\gamma \leq 0$. For such a phase to exist, $\kappa_U^{(\sigma)}(\alpha, \beta, \gamma)$ would have to be strictly greater than the corresponding mixture free energy. For a given set of $\lambda$'s the mixture arises when the square root singularities, $z_1$ and $z_2$, are equal in magnitude and they dominate any other singularities.

For $\sigma = 2$, $z_1 = \frac{w_0^{-1/\sigma}}{2}$ and $z_2 = \frac{w_2^{-1/\sigma}}{2}$. Here $w_0$ corresponds to the choice of $s_1 = s_0 = 0$ in Eq. 24, i.e. both vertices are above the interface. Similarly, $w_2$ corresponds to the choice of $s_1 = 1, s_0 = 0$ in Eq. 24, i.e. both vertices are below the interface. In a similar fashion, an exact expression can be obtained for $z_1$ and $z_2$, as functions of $\alpha, \beta, \gamma, \lambda$, for other values of $\sigma$. With these expressions, we can determine the mixture free energy by constraining $z_1 = z_2$, assuming $z_1 = \min\{\log|z_1|, \log|z_2|, \ldots, \log|z_{2+n_r}|\}$, and then solving for $\kappa_U^{(\sigma)}(\alpha, \beta, \gamma)$ in Eq. 28. Thus, for $\sigma = 2$, the *constrained limiting mixture free energy* of order 2 is equal to

$$\kappa_{\text{mix}}^{(2)}(\alpha, \beta) = \log 2 + \min_{g,\lambda}\left[-q^{(\sigma)}(\lambda) + \frac{1}{\sigma}\log w_2 + \frac{g}{\sigma}(\log w_0 - \log w_2)\right] \tag{29}$$

which is independent of $\gamma$ and where $g$ is a Lagrange multiplier introduced to impose the constraint that $\log z_1 = \log z_2$. In the solution, $g$ can be interpreted as the proportion of walks that are entirely above the interface and hence we expect that $g \in [0, 1]$.

For arbitrary but fixed $\sigma \geq 1$, the solution yields the constrained limiting mixture free energy of order $\sigma$ and is given by

$$\kappa_{\text{mix}}^{(\sigma)}(\alpha, \beta) = \log 2 + \frac{1}{\sigma} \sum_{m=0}^{\sigma} \binom{\sigma}{m} p^m (1-p)^{\sigma-m} \log(g e^{\alpha m} + (1-g) e^{\beta(\sigma-m)}) \tag{30}$$

where $g \in [0, 1]$ is the first solution in $[0, 1]$ to

$$1 = \sum_{m=0}^{\sigma} \binom{\sigma}{m} p^m (1-p)^{\sigma-m} \frac{e^{\alpha m}}{g e^{\alpha m} + (1-g) e^{\beta(\sigma-m)}}. \tag{31}$$

Given any $\gamma$ and any $\alpha, \beta > 0$, our goal is to find a choice of $\sigma$ such that $\kappa_U^{(\sigma)}(\alpha, \beta, \gamma) > \kappa_{\text{mix}}^{(\sigma)}(\alpha, \beta)$. To investigate this we consider lower bounds on $\kappa_U^{(\sigma)}(\alpha, \beta, \gamma)$ and determine $\sigma$ such that the lower bound is greater than $\kappa_{\text{mix}}^{(\sigma)}(\alpha, \beta)$. The lower bounds are discussed in the next section.

## 7 Lower bounds

We next explore lower bounds on the quenched average free energy, $\bar{\kappa}(\alpha, \beta, \gamma)$, with a focus on $p = 1/2$ and $\alpha \geq \beta$. By Eq. 12, any lower bound on $\bar{\kappa}(\alpha, \beta, \gamma)$ will also be a lower bound on $\kappa_U^{(\sigma)}(\alpha, \beta, \gamma)$, for any $\sigma \geq 0$.

The simplest lower bound on $\bar{\kappa}(\alpha, \beta, \gamma)$ is $\max\{d_A(\alpha), d_B(\beta)\}$ which for $p = 1/2$ and $\alpha \geq \beta$ is

$$\bar{\kappa}(\alpha, \beta, \gamma) \geq d_A(\alpha) = \log 2 + \alpha/2. \tag{32}$$

The next type of lower bound comes from exact enumeration. Using arguments as in [9, Lemma 1],

$$\bar{\kappa}(\alpha, \beta, \gamma) = \sup_n \left\langle n^{-1} \log Z_n(\alpha, \beta, \gamma | \chi) \right\rangle \geq \left\langle n^{-1} \log Z_n(\alpha, \beta, \gamma | \chi) \right\rangle = \bar{\kappa}_n(\alpha, \beta, \gamma), \tag{33}$$

for any $n \geq 0$. In Fig. 2a, we plot $\bar{\kappa}_{26}(\alpha, \alpha, 0)$ and $\kappa_{\text{mix}}^{(\sigma)}(\alpha, \alpha, 0)$ for $\sigma = 2, 4, \ldots, 12$. We see that for $\sigma = 12$, $\gamma = 0$ and $\beta = \alpha \geq \alpha^* \approx 8.35$ the lower bound exceeds the constrained limiting mixture free energy. Hence, at least for $\gamma = 0$, $\sigma = 12$ and sufficiently large $\alpha$, there will be a truly localized phase in the first quadrant along the line $\alpha = \beta$. In Fig. 2b, we plot $\bar{\kappa}_{26}(\alpha, \alpha, 0.5)$ and $\kappa_{\text{mix}}^{(\sigma)}(\alpha, \alpha, 0.5)$ for $\sigma = 2, 4, \ldots, 12$. We see that for $\sigma = 12$, $\gamma = 0.5$ and $\beta = \alpha \geq \alpha^* \approx 6.3$ the lower bound exceeds the constrained limiting mixture free energy. Hence, at least for $\gamma = 0.5$, $\sigma = 12$ and sufficiently large $\alpha$, there will be a truly localized phase in the first quadrant along the line $\alpha = \beta$.

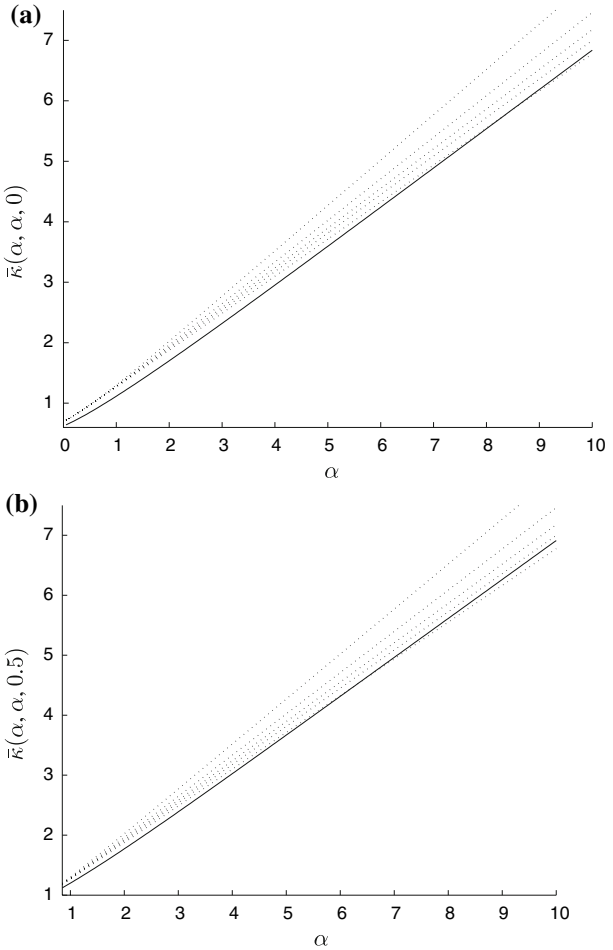


**Fig. 2** The constrained limiting mixture free energy (Eq. 29) and the exact enumeration lower bound (Eq. 33) for $n = 26$ versus $\alpha$: $\kappa_{\text{mix}}^{(\sigma)}(\alpha, \alpha, \gamma)$ (*dotted lines*) from top-right to bottom-right for $\sigma = 2, 4, 6, 8, 12$, and exact enumeration lower bound, $\bar{\kappa}_{26}(\alpha, \alpha, \gamma)$ (*solid black line*). In (**a**) $\gamma = 0$. In (**b**) $\gamma = 0.5$. Note in (**a**) that $\bar{\kappa}_{26}(\alpha, \alpha, 0) \geq \kappa_{\text{mix}}^{(12)}(\alpha, \alpha, 0)$ for all $\alpha \geq \alpha^* \approx 8.35$ and in (**b**) that $\bar{\kappa}_{26}(\alpha, \alpha, 0.5) \geq \kappa_{\text{mix}}^{(12)}(\alpha, \alpha, 0.5)$ for all $\alpha \geq \alpha^* \approx 6.3$

Another approach to obtaining a lower bound comes from considering, for each colouring $\chi$, a subset of bilateral Dyck paths such that each path in the subset has the same value, $h(\alpha, \beta, \gamma|\chi)$, for the Hamiltonian $H(\alpha, \beta, \gamma, \omega|\chi)$. In this case,

$$\begin{aligned}\bar{\kappa}_n(\alpha, \beta, \gamma) = \left\langle n^{-1} \log Z_n(\alpha, \beta, \gamma|\chi) \right\rangle &\geq \left\langle n^{-1} \log g_n(\chi) e^{h(\alpha,\beta,\gamma|\chi)} \right\rangle \\ &= \left\langle n^{-1} \log g_n(\chi) \right\rangle + \left\langle n^{-1} h(\alpha, \beta, \gamma|\chi) \right\rangle, \end{aligned} \tag{34}$$

where $g_n(\chi)$ is the number of bilateral Dyck paths, $\omega$, in the subset for which $H(\alpha, \beta, \gamma, \omega|\chi) = h(\alpha, \beta, \gamma|\chi)$. Equation 34 combined with Eq. 33 then gives a lower bound on $\bar{\kappa}(\alpha, \beta, \gamma)$.

We use a generalized version of this type of argument to obtain a lower bound which is expected to be best for any $\gamma$ and large $\alpha \gg \beta$. The goal is to investigate how good the Morita approximations are well-within the localized region. Given a colouring $\chi$, the general idea is to consider bilateral Dyck paths obtained by placing all the $A$s above, and if there is a run of 3 or more consecutive $B$s starting at an even vertex, then we allow them to behave as in an adsorption at an impenetrable surface where the surface is $y = 0$ and the walk lies in the half-space $y \leq 0$. This yields, for each $n \geq 2$, the following lower bound for $\bar{\kappa}(\alpha, \beta, \gamma)$,

$$\kappa_{\mathrm{LB}}^{(n)}(\alpha, \beta, \gamma) = \frac{1}{2}\alpha + \frac{4}{19}\beta + \frac{3}{38}\gamma + \frac{9}{38}\sum_{i=1}^{n}\left(\frac{1}{4}\right)^{i}\log\left(Z_i^a(\gamma - \beta)\right) + \sum_{i=1}^{n}\left(c_1 r_1^i + c_2 r_2^i\right)\log d_i, \tag{35}$$

where $Z_i^a(x)$ is the homopolymer partition function for adsorption at an impenetrable surface for Dyck paths of length $2i$ with surface interaction energy $x$ (see [7], Sect. 3.2) and $d_i$ is the number of Dyck paths of length $2i$. The term, $c_1 r_1^i + c_2 r_2^i$, is known exactly for each $i$ as it can be determined from the probability that the first run of 3 or more consecutive $B$s starting at an even vertex occurs at the $i$th step of the walk. In fact, the constants (up to 6 significant decimal places) are given by $c_1 = 0.004437$, $r_1 = 0.890388$, $c_2 = -0.001147$, $r_2 = -0.140388$. Similarly the other constant coefficients in Eq. 35 can be determined from the colour distribution. An explicit formula for $d_n$ can be determined from the Dyck path generating function $D(z) = \sum_n d_n z^n = \frac{1-\sqrt{1-4z}}{2z}$ (see [15]).

## 8 Results for $p = 1/2$

For fixed $\gamma \leq \gamma_L^{(1)} = 2\log 2$, any $\alpha$ and $\beta \leq \beta_1(\alpha, \gamma)$, the Morita approximation free energy $\kappa_U^{(\sigma)}(\alpha, \beta, \gamma) = d_A(\alpha) = \alpha/2 + \log 2$ for all $\sigma \geq 1$ (by [11]). Therefore we confine our discussion of bounds on the limiting quenched average free energy, $\bar{\kappa}(\alpha, \beta, \gamma)$, to the region $\beta > \beta_1(\alpha, \gamma)$. Even though the delocalized phase boundary does not change as the order of the Morita approximation increases, the Morita approximation bounds on the limiting quenched average free energy do improve. In particular, for large enough $\gamma \leq \gamma_L^{(1)}$ and high enough Morita approximation order $\sigma$, we will show that the whole localized region is consistent with property (ii), i.e. the limiting density of visits is strictly positive and hence the mixture region disappears along the $\alpha = \beta$ line. The evidence from Figs. 2a and b, where the exact enumeration lower bound $\bar{\kappa}_{26}(\alpha, \alpha, \gamma)$ is larger than the mixture free energy $\kappa_{\mathrm{mix}}^{(12)}(\alpha, \alpha, \gamma)$ for large $\alpha$, suggests that there is a $\sigma \leq 12$ that may be sufficient. We explore this further next.

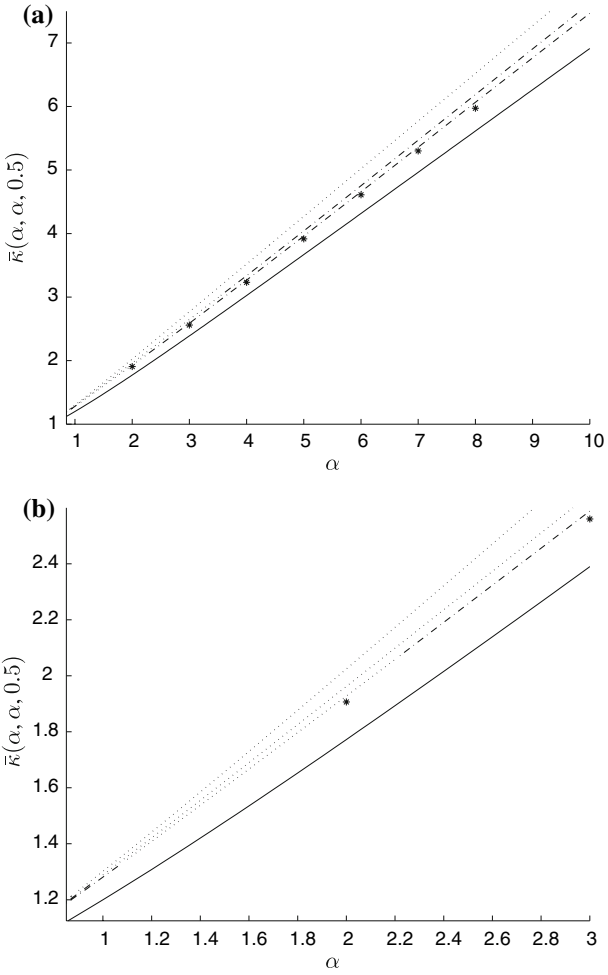


**Fig. 3** For $\gamma = 0.5$ and $\beta = \alpha$, bounds on $\bar{\kappa}(\alpha, \alpha, 0.5)$ are shown: Morita upper bounds, $\kappa_U^{(\sigma)}(\alpha, \alpha, 0.5)$ (*top three curved lines*) for $\sigma = 2, 4, 6$, $\kappa_U^{(8)}(\alpha, \alpha, 0.5)$ (*), exact enumeration lower bound $\bar{\kappa}_{26}(\alpha, \beta = \alpha, \gamma = 0.5)$ (*solid bottom line*). In (**b**) A closer view is shown

In Fig. 3a we plot the Morita upper bounds ($\kappa_U^{(\sigma)}$) and our best lower bound, the exact enumeration lower bound ($\bar{\kappa}_{26}$), along the $\alpha = \beta$ line for $\gamma = 0.5$. Figure 3b zooms into Fig. 3a for small values of $\alpha$. The top curve is $\kappa_U^{(2)}$, which consists of a truly localized section (dash-dot line for $\alpha \leq 0.87298039$) and a mixture section (dotted line for $\alpha > 0.87298039$). The next curve (from top to bottom) is $\kappa_U^{(4)}$, which consists of two truly localized sections (dash-dot lines for $\alpha \leq 0.9528422$ and $\alpha \geq 3.5338275$) and a mixture section (dotted line for $0.9528422 < \alpha < 3.5338275$). The third curve (from top to bottom) is $\kappa_U^{(6)}$, which consists of two truly localized sections (dash-dot lines for $\alpha \leq 1.0704566$ and $\alpha \geq 2.213918$) and a mixture section (dotted line for $1.0704566 < \alpha < 2.213918$). The upper bounds $\kappa_U^{(\sigma)}$ for $\sigma \geq 8$ require a lot of

**Table 1** For $\gamma = 0.5$ and $\beta = \alpha$, bounds on $\bar{\kappa}(\alpha, \alpha, 0.5)$ at $\alpha = 2, 4, \ldots, 10$ are listed by the method used (bnd) and the order ($\sigma$)

| $\sigma^{\text{bnd}}$ | $\alpha = 2$ | 4 | 6 | 8 | 10 |
|---|---|---|---|---|---|
| $1^{[2]}$ | 2.12692 | 4.01814 | 6.00247 | 8.00033 | 10.00004 |
| $2^{Morita}$ | 2.02439 | 3.51994 | 5.01986 | 6.51986 | 8.01986 |
| $4^{Morita}$ | 1.96212 | 3.33706 | 4.75348 | 6.18781 | 7.62488 |
| $6^{Morita}$ | 1.92765 | 3.26712 | 4.65732 | 6.06540 | 7.46704 |
| $8^{Morita}$ | 1.90636 | 3.23245 | 4.60677 | 5.97210 | |
| $26^{LBee}$ | 1.77219 | 3.02470 | 4.31546 | 5.61333 | 6.91230 |
| $400^{LB}$ | 1.680917 | 2.940582 | 4.2032309 | 5.466319 | 6.72946 |

The case $1^{[2]}$ is based on results of [7], the Morita bounds for $\sigma = 2, 4, 6, 8$ are based on Eq. 28; *LBee* is an exact enumeration lower bound as in Eq. 33; *LB* is the lower bound from Eq. 35

computation time and hence we only plot a few points for $\kappa_U^{(8)}$. The points marked by a (*), just below $\kappa_U^{(6)}$, correspond to $\kappa_U^{(8)}$, which consists entirely of a truly localized free energy term (the same occurs for higher $\sigma$ and higher $\gamma$ values). Figure 2b showed that that the mixture disappeared for $\sigma \geq 12$ and large enough $\alpha$ (by comparing $\bar{\kappa}_{26}$ against $\kappa_{\text{mix}}^{(\sigma)}$) and now we see that in fact it ceases to exist for $\sigma \geq 8$ and any $\alpha$. Hence, the whole line $\alpha = \beta$ is truly localized and is therefore consistent with property (ii), i.e. the limiting density of visits is strictly positive. The upper and lower bounds for various values of $\sigma$ are shown in Table 1 along the $\alpha = \beta$ line for $\gamma = 0.5$. It is clear from Figs. 3a and b and from Table 1 that the Morita approximation upper bounds $\kappa_U^{(\sigma)}$ improve as $\sigma$ increases.

We note in general that for $\sigma \geq 4$ the calculations are all numerical and hence, for example, although we report above that $\kappa_U^{(\sigma)} = \kappa_{\text{mix}}^{(\sigma)}$ in intermediate regions of $\alpha$ for $\sigma = 4, 6$, we have not ruled out the possibility that the pole (characterizing the truly localized phase) is so close to the square root singularity (characterizing the mixture) that they are numerically indistinguishable.

Along the $\alpha = \beta$ line, the upper and lower bounds do not get very close together. However, the bounds are much better in other parts of the localized region. For example, Fig. 4 presents the case of fixed $\beta = 2.5$ and fixed $\gamma = 0.5$. The Morita upper bounds ($\kappa_U^{(\sigma)}$) and the best lower bound, $\kappa_{\text{LB}}^{(400)}$, are shown. The top curve is $\kappa_U^{(2)}$, which consists entirely of a mixture. The next curve (from top to bottom) is $\kappa_U^{(4)}$, which consists of a mixture section (dotted line for $\alpha < 5.286769$) and a truly localized section (dash-dot line for $\alpha \geq 5.286769$. The third curve (from top to bottom) is $\kappa_U^{(6)}$, which consists entirely of a truly localized phase (the same occurs for higher $\sigma$ values). The points marked by a (*), just below $\kappa_U^{(6)}$, correspond to $\kappa_U^{(8)}$, which consists entirely of a truly localized phase. The upper and lower bounds for various values of $\sigma$ with a fixed value of $\beta = 2.5$ and fixed $\gamma = 0.5$ are shown in Table 2. It is clear again from Fig. 4 and Table 2 that the Morita approximation (upper bound) improves as $\sigma$ increases, and that the upper bound, $\kappa_U^{(8)}$, and lower bound, $\kappa_{\text{LB}}^{(400)}$, are very close together for large $\alpha$.

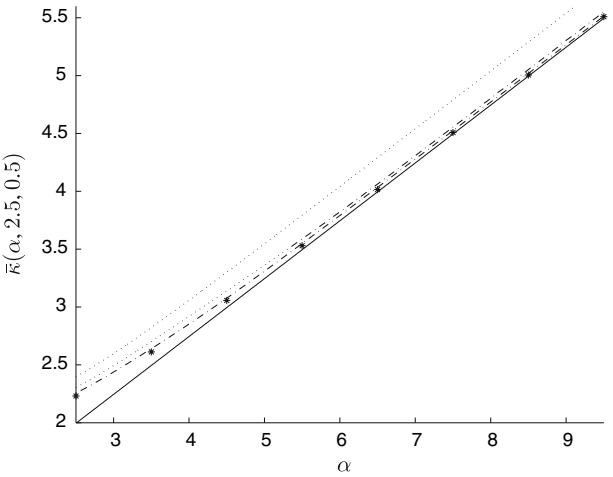


**Fig. 4** For $\gamma = 0.5$, $\beta = 2.5$, bounds on $\bar{\kappa}(\alpha, 2.5, 0.5)$ are shown: Morita upper bounds, $\kappa_U^{(\sigma)}(\alpha, 2.5, 0.5)$ (*top three curved lines*) for $\sigma = 2, 4, 6$, $\kappa_U^{(8)}(\alpha, 2.5, 0.5)$ (*), lower bound $\bar{\kappa}_{\mathrm{LB}}(\alpha, 2.5, 0.5)$ (*solid bottom line*)

**Table 2** For $\gamma = 0.5$ and $\beta = 2.5$, bounds on $\bar{\kappa}(\alpha, \beta = 2.5, \gamma = 0.5)$ at $\alpha = 2.5, 3.5, \ldots, 9.5$ are listed by the method used (bnd) and the order ($\sigma$)

| $\sigma^{\mathrm{bnd}}$ | $\alpha = 2.5$ | 3.5 | 4.5 | 5.5 | 6.5 | 7.5 | 8.5 | 9.5 |
|---|---|---|---|---|---|---|---|---|
| $1^{[2]}$ | 2.5788 | 3.0556 | 3.5474 | 4.0445 | 4.5434 | 5.0430 | 5.5429 | 6.0428 |
| $2^{Morita}$ | 2.3965 | 2.8228 | 3.3009 | 3.7936 | 4.2910 | 4.7900 | 5.2897 | 5.7895 |
| $4^{Morita}$ | 2.3044 | 2.7023 | 3.1392 | 3.5885 | 4.0628 | 4.5544 | 5.0515 | 5.5505 |
| $6^{Morita}$ | 2.2555 | 2.6401 | 3.0760 | 3.5490 | 4.0343 | 4.5245 | 5.0184 | 5.5144 |
| $8^{Morita}$ | 2.2308 | 2.6117 | 3.0567 | 3.5299 | 4.0154 | 4.5087 | 5.0053 | 5.5035 |
| $400^{LB}$ | 1.9951 | 2.4951 | 2.9951 | 3.4951 | 3.9951 | 4.4951 | 4.9951 | 5.4951 |
| $26^{LBee}$ | 2.0773 | 2.4371 | 2.8604 | 3.3132 | 3.7799 | 4.2534 | 4.7304 | 5.2091 |

The case $1^{[2]}$ is based on results of [7], the Morita bounds for $\sigma = 2, 4, 6, 8$ are based on Eq. 28; *LBee* is an exact enumeration lower bound as in Eq. 33; *LB* is a lower bound based on Eq. 35

## 9 Conclusions

We have developed a direct renewal approach for obtaining Morita approximations of arbitrary even order. These approximations lead, with increasing order, to a sequence of improved upper bounds on the limiting quenched average free energy of bilateral Dyck path localization. We have also obtained explicit expressions for the corresponding constrained limiting mixture free energies, and we have obtained lower bounds on the limiting quenched average free energy of bilateral Dyck path localization.

With these results, for $p = 1/2$, we are able to show that it is possible to eliminate the mixture phase from the order $\sigma$ Morita approximation phase diagram along the line $\alpha = \beta$ for sufficiently high $\gamma$ and $\sigma$. We have also shown that well-within the localized region, one can obtain the limiting quenched average free energy very precisely

(to within $\pm 0.01$) based on the Morita approximation of order 8 and the lower bound in Eq. 35 with $n = 400$.

We have investigated properties of the mixture phase boundaries for various values of $\alpha, \beta, \gamma$ (including $\gamma < 0$) and for Morita approximations of order $2 \leq \sigma \leq 12$. Further results from these investigations will be reported in a future paper. We are still investigating which order of Morita approximation is sufficient to eliminate the mixture from the line $\alpha = \beta$ for all $\gamma$.

**Acknowledgements** The authors wish to acknowledge helpful conversations with Stu Whittington and Enzo Orlandini. We also wish to acknowledge financial support from the University of Saskatchewan and NSERC of Canada, and computer resource support from WestGrid. The authors also greatly appreciated the hospitality of the Chemical Physics Theory Group, Department of Chemistry, University of Toronto, when some of the results were obtained.

## References

1. J.S. Phipps, R.M. Richardson, T. Cosgrove, A. Eaglesham, Neutron reflection studies of copolymers at the hexane/water interface. Langmuir **9**, 3530–3537 (1993)
2. B.J. Clifton, T. Cosgrove, R.M. Richardson, A. Zarbakhsh, J.R.P. Webster, The structure of block copolymers at the fluid/fluid interface. Physica. B. **248**, 289–296 (1998)
3. C.E. Soteros, S.G. Whittington, The statistical mechanics of random copolymers. J. Phys. A. **37**, R1–R47 (2004)
4. R. Martin, M.S. Causo, S.G. Whittington, Localization transition for a randomly coloured self-avoiding walk at an interface. J. Phys. A. **33**, 7903–7918 (2000)
5. N. Madras, S.G. Whittington, Localization of a random copolymer at an interface. J. Phys. A. **36**, 923–938 (2003)
6. J. Alvarez, E. Orlandini, C.E. Soteros, S.G. Whittington, Higher order Morita approximations for random copolymer adsorption. J. Phys. A: Math. Theor. **40**, F289–F298 (2007)
7. E. Orlandini, A. Rechnitzer, S.G. Whittington, Random copolymers and the Morita approximation: polymer adsorption and polymer localization. J. Phys. A. **35**, 7729–7751 (2002)
8. G. Iliev, A. Rechnitzer, S.G. Whittington, Random copolymer localization and the Morita approximation. J. Phys. A. **38**, 1209–1223 (2005)
9. E.W. James, C.E. Soteros, S.G. Whittington, Localization of a random copolymer at an interface: an untethered self-avoiding walk model. J. Phys. A. **36**, 11187–11200 (2003)
10. E.J. Janse van Rensburg, Statistical mechanics of directed models of polymers in the square lattice. J. Phys. A. **36**, R11–R61 (2003)
11. F. Caravenna, G. Giacomin, On constrained annealed bounds for pinning and wetting models. Elect. Comm. Probab. **10**, 179–189 (2005)
12. T. Morita, Statistical mechanics of quenched solid solutions with application to magnetically dilute alloys. J. Math. Phys. **5**, 1401–1405 (1964)
13. R.M. Mazo, Free energy of a system with random elements. J. Chem. Phys. **39**, 1224–1225 (1963)
14. R. Kühn, Equilibrium ensemble approach to disordered systems. Z. Phys. B. **100**, 231–242 (1996)
15. S.K. Lando, *Lectures on Generating Functions* (American Mathematical Society, Providence, 2003)